

# Adaptive Step Duration for Precise Foot Placement: Achieving Robust Bipedal Locomotion on Terrains with Restricted Footholds

Zhaoyang Xiang<sup>1</sup>, Victor Paredes<sup>1</sup>, Guillermo A. Castillo<sup>2</sup>, and Ayonga Hereid<sup>1</sup>

**Abstract**—Traditional one-step preview planning algorithms for bipedal locomotion struggle to generate viable gaits when walking across terrains with restricted footholds, such as stepping stones. To overcome such limitations, this paper introduces a novel multi-step preview foot placement planning algorithm based on the step-to-step discrete evolution of the Divergent Component of Motion (DCM) of walking robots. Our proposed approach adaptively changes the step duration and the swing foot trajectory for optimal foot placement under constraints, thereby enhancing the long-term stability of the robot and significantly improving its ability to navigate environments with tight constraints on viable footholds. We demonstrate its effectiveness through various simulation scenarios with complex stepping-stone configurations and external perturbations. These tests underscore its improved performance for navigating foothold-restricted terrains, even with external disturbances.

## I. INTRODUCTION

Bipedal robots are designed to collaborate with humans while navigating complicated and crowded human environments built for our daily lives. These environments often restrict the robot's viable footholds, requiring the robot to be able to adaptively plan its gaits in real-time so that the foot always lands in given limited areas. In the literature on bipedal locomotion, such limited areas are often regarded as stepping stones, as illustrated in Fig. 1. Many dynamic walking algorithms fail to successfully tackle stepping stones as they often assume the foot can be placed anywhere within the allowable workspace of the swing foot. A noticeable exception in the literature is the use of full-body trajectory optimization with foothold constraints. For example, a library of gaits can be generated offline with a set of fixed stepping-stone profiles, and then interpolated online given the real-time feedback of the next foot placement area [1] or adapted through an online MPC with a whole-body controller [2]. However, the adaptability of such approaches is limited due to the difficulty in optimizing a full-body trajectory in real-time for any given stepping stone profile.

A popular approach to mitigate the complexity of robot dynamics in gait planning is using reduced-order template models to represent the critical progression of bipedal robots during locomotion. The most commonly used model, the linear inverted pendulum model (LIPM), describes the center of mass (CoM) dynamics with an inverted pendulum with

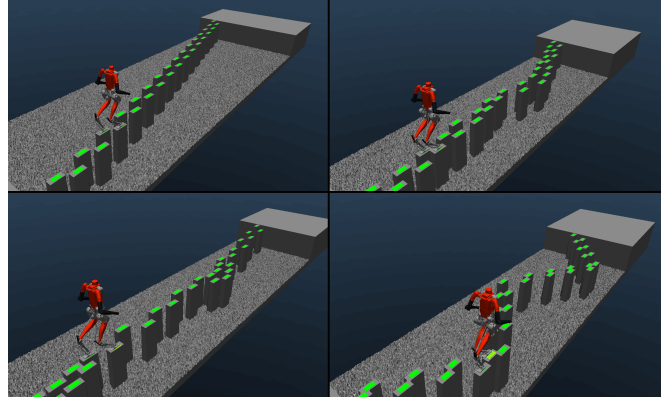


Fig. 1. Digit robot stably walks across four challenging stepping stone scenarios in MuJoCo simulation by dynamically adjusting both step duration and stepping locations.

a constant height [3]–[6]. To provide a criterion for gait stability of pendulum-based CoM dynamics models, the capturability [7] and the Divergent Component of Motion (DCM) [8] decouple the stable and unstable dynamics based on the viable states (i.e., states that do not lead to falling). Those analyses also show that a variable step duration can increase the range of viable states and allow robots to prevent falling by taking faster and wider steps. However, such a time-varying variable usually leads to nonlinear and non-convex planning problems, which require heavy computing resources and thus impede its implementation in online controllers. Griffin *et al.* formulate a continuous-time MPC for the time-varying DCM as a mixed-integer quadratically constrained quadratic program (MIQCP) that shows good resistance to force perturbations but suffers from slow online solving (average about 72 ms) [9].

The decoupling of the stable and unstable dynamics through DCM allows the gait planner to regulate both stepping position and timing conveniently. Khadiv *et al.* introduce the DCM offset to represent the viability bounds of the LIPM model and formulate the desired step position and step duration into an online quadratic programming (QP) [10]. Their foot placement planner finds an optimal foot placement to ensure bounded viable states, thus improving perturbation resistance. There are also extended works for more complicated stepping strategies [11] and more challenging walking perturbation [12], which implies their potential application in bipedal locomotion on stepping stones. Nonetheless, these approaches depend on one-step preview planning, in which the gait features are determined without considering the

\*This work was supported in part by the National Science Foundation under grant FRR-21441568.

<sup>1</sup>Mechanical and Aerospace Engineering, The Ohio State University, Columbus, OH, USA. (xiang.295, paredescauna.1, hereid.1)@osu.edu.

<sup>2</sup>Electrical and Computer Engineering, The Ohio State University, Columbus, OH, USA; castillomartinez.2@osu.edu

restrictions on future foothold locations. Consequently, this limits their adaptability to traverse randomly placed stepping stones.

In this work, we develop a multi-step preview gait planning approach to improve the overall stability and long-horizon viability of bipedal walking, even in the presence of severe constraints on the footholds. We introduce a multiple-step Model Predictive Control (MPC) formulation to adjust step durations and stepping positions while walking over randomly located stepping stones. Our formulation uses the modified form of DCM based on the contact angular momentum rather than the linear velocity of the base. This is inspired by the improved performance of the angular momentum-based linear inverted pendulum (ALIP) in bipedal locomotion on various terrains due to better approximation of robot dynamics [13]–[15]. We validated the proposed approach with Digit humanoid in simulation under various types of stepping stone profiles and perturbations. Compared with the one-step preview algorithm in [10], our planner achieves more robust bipedal locomotion over challenging scenarios.

The remainder of the paper is organized as follows: Section II introduces the modified DCM formulation, and Section III proposes a multi-step preview planner that adaptively changes step durations to remain stable on stepping stones. Section IV discusses the modification in low-level task space tracking controller in response to adaptive step durations. Section V shows the simulation results with the Digit robot, and finally Section VI briefly concludes the contributions and discusses future plans.

## II. DIVERGENT COMPONENT OF MOTION ANALYSIS OF BIPEDAL LOCOMOTION

This section introduces the modified DCM formulation based on the contact angular momentum-based linear inverted pendulum (ALIP) model. We also explicitly discuss the bounds of step positions and durations for stable locomotion.

### A. Center of Mass Dynamics of Bipedal Robots

We consider the ALIP model on a flat ground with an underactuated single-support phase and an instantaneous double-support phase [13]. Using  $x_c, y_c, z_c$  to denote the CoM position in the right-handed contact point frame, the ALIP dynamics are given by

$$\begin{aligned} \dot{x}_c &= \frac{L^y}{mz_c}, & \dot{y}_c &= -\frac{L^x}{mz_c}, \\ \dot{L}^x &= -mg y_c, & \dot{L}^y &= mg x_c, \end{aligned} \quad (1)$$

where  $z_c$  is the constant CoM height,  $L^x, L^y$  are the  $x, y$ -component of the angular momentum about the contact point (i.e., contact angular momentum),  $m$  is the mass of the robot, and  $g$  is the gravitational acceleration constant. Compared to the LIPM described in [3], the ALIP model uses the contact angular momentum  $L^x, L^y$  instead of the linear velocities of the CoM. This change reduces the mismatch between the template model and the real robot state as it only assumes

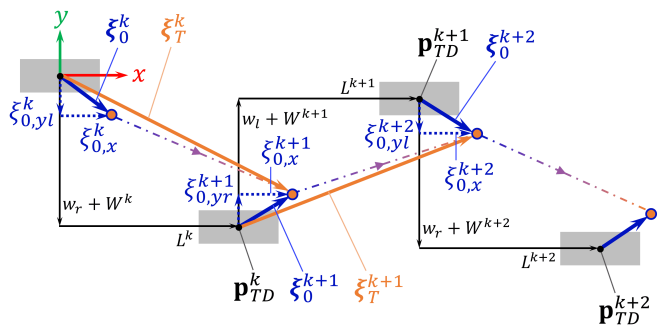


Fig. 2. Schematic view of the DCM evolution with step positions and footprints. During the  $k$ -th step, the DCM evolves from  $\xi_0^k$  to  $\xi_T^k$  and is reset to  $\xi_0^{k+1}$  in the new contact frame after the touch-down.

the centroidal angular momentum is zero instead of the rate of change of the centroidal angular momentum is zero [13].

### B. Discrete Dynamics of the initial DCM

The ALIP dynamics in (1) can be transformed into a system that separates the stable and unstable parts of its dynamics, where the latter is its Divergent Component of Motion [8]. Using the states of the ALIP model, the DCM  $\xi = [\xi_x, \xi_y]^T$  in the contact frame is given by

$$\xi = \begin{bmatrix} x_c \\ y_c \end{bmatrix} + \frac{1}{\lambda} \frac{1}{mz_c} \begin{bmatrix} L^y \\ -L^x \end{bmatrix}, \quad \lambda = \sqrt{\frac{g}{z_c}}. \quad (2)$$

Substituting the ALIP dynamics (1) into (2), we can obtain the DCM dynamics as  $\dot{\xi} = \lambda \xi$  with the solution

$$\xi(t) = \xi_0 e^{\lambda t}, \quad t \in [0, T], \quad (3)$$

where  $t$  is the elapsed time (or relative time) from the beginning of the current swing phase,  $T$  is the step duration, and  $\xi_0$  is the initial DCM at  $t = 0$ . During a walking step, the DCM  $\xi(t)$  increase exponentially over the time  $t$  and is reset to an initial value after a swing foot touch-down due to the update of the contact frame (see Fig. 2). Suppose that the current step is the  $k$ -th step ( $k \in \mathbb{N}^+$ ),  $\xi_0^k$  and  $\xi_T^k$  are the initial and final value of the DCM of the  $k$ -th step, and  $\xi_0^{k+1}$  is the initial value of the  $(k+1)$ -th step that is also referred to as the DCM offset at the end of the  $k$ -th step in [10]. Then, the reset map of the DCM is given by

$$\xi_0^{k+1} = \Delta_k(\xi_0^k) = \xi_T^k - \mathbf{p}_{TD}^k = \xi_0^k e^{\lambda T^k} - \mathbf{p}_{TD}^k, \quad (4)$$

where  $\mathbf{p}_{TD}^k = [x_{TD}^k, y_{TD}^k]^T$  is the  $k$ -th step position in the current contact frame and  $T^k$  is the  $k$ -th step duration.

Note that the DCM is innately decoupled in  $x$ - and  $y$ -direction. For a 3-D bipedal model, there will be an alternating step width  $w_{l/r}$  for the left or right swing foot even if the robot is stepping in place. Thus, we define the lateral step position  $y_{TD}^k := w_{l/r} + W^k$ , where  $w_{l/r}$  is a fixed step width of the left or right swing foot during in-place lateral walking, and  $W^k$  is an offset to  $w_{l/r}$  that accounts for the actual lateral movement. That is, given a fixed step width  $w > 0$ , the signed step width for the left swing foot is  $w_l = w > 0$  and for the right  $w_r = -w < 0$ . For instance,

Fig. 2 shows a rightward walking in the  $y$ -direction with  $W^k < 0$ .

For a periodic gait with a constant step position  $\mathbf{p}_{TD}^k = [L, w_{l/r} + W]^T$  and duration  $T^k = T$ , the nominal value of the initial DCM  $\xi_{0,\text{nom}}$  can be derived from (4) as

$$\xi_{0,\text{nom}} = \begin{bmatrix} \xi_{0,x,\text{nom}} \\ \xi_{0,y/r,\text{nom}} \end{bmatrix} = \begin{bmatrix} \frac{L}{e^{\lambda T} - 1} \\ \frac{w_{l/r}}{e^{\lambda T} + 1} + \frac{W}{e^{\lambda T} - 1} \end{bmatrix}, \quad (5)$$

where  $\xi_{0,y/r,\text{nom}}$  of the left or right swing foot are solved by considering two consecutive steps (i.e., one cycle of lateral walking).

In the  $x$ -direction, given a bounded set  $\mathcal{D}$  of allowable step position and  $\mathcal{T}$  of allowable step duration, we can obtain a bounded set  $\mathcal{X}$  of the nominal initial DCM computed by the values in  $\mathcal{D}$  and  $\mathcal{T}$  using (5), i.e.,  $\xi_{0,x,\text{nom}}(L, T) : \mathcal{D} \times \mathcal{T} \rightarrow \mathcal{X}$ ,  $\forall L \in \mathcal{D}, T \in \mathcal{T}$ . Each element in this set represents a particular periodic walking gait corresponding to a foot placement  $(L, T)$ , which leads to the following proposition.

**Proposition.** *Given appropriate allowable sets  $\mathcal{D}^k, \mathcal{T}^k \subset \mathbb{R}$  of the  $k$ -th step, for any initial DCM  $\xi_{0,x}^k$  in  $\mathcal{X}^k$  that evolves once into  $\xi_{0,x}^{k+1}$  using (4), there exists at least one allowable foot placement  $(L^k, T^k)$  such that  $\xi_{0,x}^{k+1}$  still remains in  $\mathcal{X}^k$ .*

*Proof.* Let  $\mathcal{D}^k = [L_{\min}, L_{\max}]$  with  $L_{\min} < 0 < L_{\max}$  and  $\mathcal{T}^k = [T_{\min}, T_{\max}]$  with  $0 < T_{\min} < T_{\max}$ , the bound of  $\mathcal{X}^k$  is given by (5) as

$$\begin{aligned} \xi_{0,x,\min} &= \frac{L_{\min}}{e^{\lambda T_{\min}} - 1} < 0, \\ \xi_{0,x,\max} &= \frac{L_{\max}}{e^{\lambda T_{\min}} - 1} > 0. \end{aligned} \quad (6)$$

For any  $\xi_{0,x}^k \in \mathcal{X}^k$ , the evolved initial DCM by the foot placement  $(L^k, T^k)$  is  $\xi_{0,x}^{k+1} = \xi_{0,x}^k e^{\lambda T^k} - L^k$ . Thus, by choosing  $(L^k, T^k)$  as  $(L_{\min}, T_{\min})$  or  $(L_{\max}, T_{\min})$ ,  $\xi_{0,x}^{k+1}$  can be bounded as

$$\begin{aligned} \xi_{0,x}^{k+1} &\geq \frac{L_{\min}}{e^{\lambda T_{\min}} - 1} e^{\lambda T_{\min}} - L_{\min} = \xi_{0,x,\min}, \\ \xi_{0,x}^{k+1} &\leq \frac{L_{\max}}{e^{\lambda T_{\min}} - 1} e^{\lambda T_{\min}} - L_{\max} = \xi_{0,x,\max}, \end{aligned} \quad (7)$$

i.e.,  $\xi_{0,x}^{k+1}$  remains in  $\mathcal{X}^k$ .  $\square$

A similar result also applies to the  $y$ -direction, where there exist two consecutive foot placements such that any initial DCM  $\xi_{0,y/r}^k$  has a bounded evolution. The bound of such  $\mathcal{X}$  is referred to as the  $\infty$ -step capturability bound  $d_\infty$  (or viability bound) in [7] that theoretically distinguishes the stable walking gaits from the unstable ones, and such a bounded (or viable) evolution of the DCM represents a walking gait that never falls. Moreover, it can be shown that the evolution of the initial DCM in the interior of  $\mathcal{X}$  can increase the viability margin, which implies a more "stable" walking system [16].

For pedal robotic walking without terrain and physical (e.g., leg length) constraints, the allowable sets of each foot placement are almost identical (though symmetric in the

$y$ -direction). Thus, we can always find at least one stable gait that converges to a periodic one given an appropriate initial DCM  $\xi_0^1$ . However, even if the allowable sets of foot placements are constrained, it is still possible to find such stable gaits. This intuitively inspires a foot placement strategy on restricted footholds.

### III. SWING FOOT PLACEMENT PLANNING VIA DISCRETE MODEL PREDICTIVE CONTROL

The main contribution of this work is to design a foot placement planner on the stepping stones with high accuracy and resistance to external perturbations. The stepping stones can be modeled as a sequence of bounds on each step position, which leads to significant constraints on the dynamic walking. Therefore, multiple future steps must be considered to find a stable walking gait by exploiting the viable evolution of the initial DCM with variable step duration.

To simplify the denotation, we define  $\mathbf{z}^k := \xi_0^{k+1}$ ,  $\mathbf{u}^k := \mathbf{p}_{TD}^k$ , and  $\sigma^k := e^{\lambda T^k}$ , then the step-to-step discrete dynamics of the initial DCM by (4) is given by

$$\mathbf{z}^k = \sigma^k \mathbf{z}^{k-1} - \mathbf{u}^k, \quad k = 1, 2, \dots, \quad (8)$$

where  $\mathbf{z}^0 = \xi_0^1 = \xi(0)$  is the initial DCM of the current step.

We now propose an MPC formulation based on the discrete dynamics (8) that minimizes the errors between the gait parameters  $(\mathbf{z}^k, \sigma^k, \mathbf{u}^k)$  and their desired values for multiple future steps. The design of the optimization constraints and objectives on the decision variables are as follows:

1) **Step Position:** For the Digit robot model with under-actuated ankles and flat feet, we define the step position  $\mathbf{u}^k$  as the geometric center at the bottom of each stance foot. A stepping stone profile is given as a sequence of fixed positions in the world frame, while the robot states and variables such as the DCM and the step position are defined in each contact frame. Given the preview of next  $N$  stepping stones in the current contact frame, the target is to minimize the error between the future step position  $\mathbf{u}^k$  and stone position  $\mathbf{p}_{\text{stone}}^k$  for  $k = \{1, 2, \dots, N\}$ . Thus, the desired values of each step position are computed as

$$\mathbf{u}_{\text{des}}^k = \begin{cases} \mathbf{p}_{\text{stone}}^1, & k = 1 \\ \mathbf{p}_{\text{stone}}^k - \mathbf{p}_{TD,\text{ccf}}^{k-1}, & k = 2, \dots, N \end{cases}, \quad (9)$$

where  $\mathbf{p}_{TD,\text{ccf}}^{k-1}$  should be the actual step position of the future  $(k-1)$ -th step in the current contact frame. Since  $\mathbf{p}_{TD,\text{ccf}}^{k-1}$  are unknown during the current step, we use the previous planning results to approximate their actual values, which are iteratively updated inside the planner. In practice, if the planner has not returned the first result right after a touchdown, we then use the position of the  $(k-1)$ -th stone instead.

Moreover, the bound on each step position is defined as a rectangular area around the  $\mathbf{p}_{\text{stone}}^k$  that represents the physical dimension of each stepping stone.

2) **Step Duration:** Since we emphasize the accuracy of the step position and viability of the walking gait, we make the step duration a slack variable to relax the problem. We choose a constant nominal value  $T_{\text{des}}^k = T_{\text{nom}}$  and a constant

bound  $[T_{min}, T_{max}]$  for  $T^k$ , and assign a small weight for the step duration term  $\sigma^k$  in the cost function.

3) **Initial DCM**: The desired value of the initial DCM  $\mathbf{z}^k$  are computed using (5) by substituting the desired values of the step position and duration of the  $k$ -th step. The bounds of the initial DCM are obtained using the mechanical limits of the robot model, which rules out all the infeasible states that lead to the robot falling. However, these bounds alone do not guarantee foot placements that can yield viable states for all the given stepping stones. Therefore, we choose an appropriately high weight in the cost term for each  $\mathbf{z}^k$  to track the desired value. This works as a soft constraint to enforce a viable evolution of the initial DCM through multiple steps.

Moreover, since this foot placement planner runs multiple times during a step, we use the measured value of the instantaneous DCM  $\xi_{mea}(\tilde{t})$  to estimate the initial DCM of the current step  $\mathbf{z}^0$  by computing it backward using (3):

$$\mathbf{z}^0 = \xi_0^1 = \xi_{mea}(\tilde{t})e^{-\lambda\tilde{t}}, \quad (10)$$

where  $\tilde{t} \in [0, T^1]$  is the current relative time of the step so that  $\mathbf{z}^0$  is also iteratively updated using the robot states.

4) **Discrete MPC Formulation**: Combining (8), (9), (10), and other constraints defined above, we now formulate the discrete MPC problem as follows:

$$\begin{aligned} \arg \min_{\mathbf{z}^k, \sigma^k, \mathbf{u}^k} \quad & \sum_{k=1}^N \beta^k \left( \alpha_z^k \|\mathbf{z}^k - \mathbf{z}_{des}^k\|^2 \right. \\ & + \alpha_\sigma^k |\sigma^k - \sigma_{des}^k|^2 \\ & \left. + \alpha_u^k \|\mathbf{u}^k - \mathbf{u}_{des}^k\|^2 \right) \\ \text{s. t.} \quad & \mathbf{z}^k = \sigma^k \mathbf{z}^{k-1} - \mathbf{u}^k, \\ & \begin{bmatrix} z_{x,min} \\ z_{yl/r,min} \end{bmatrix} \leq \mathbf{z}^k \leq \begin{bmatrix} z_{x,max} \\ z_{yl/r,max} \end{bmatrix}, \\ & e^{\lambda T_{min}} \leq \sigma^k \leq e^{\lambda T_{max}}, \\ & \begin{bmatrix} u_{x,min}^k \\ u_{yl/r,min}^k \end{bmatrix} \leq \mathbf{u}^k \leq \begin{bmatrix} u_{x,max}^k \\ u_{yl/r,max}^k \end{bmatrix}. \end{aligned}$$

where  $k = \{1, 2, \dots, N\}$ , and we use the weights  $\alpha_{\square}^k$  and  $\beta^k$  to represent soft constraints on the decision variable such that:  $\alpha_{\square}^k$  assigns relative weights on  $(\mathbf{z}^k, \sigma^k, \mathbf{u}^k)$  for the  $k$ -th future step as we discussed above;  $\beta^k$  is a decaying weight on each future step, addressing the importance of previewing earlier future steps, especially the imminent next one.

Since the discrete dynamics of DCM (8) takes a bilinear form about the decision variables  $(\mathbf{z}^k, \sigma^k, \mathbf{u}^k)$ , we arrive at a nonlinear programming (NLP) problem. It takes considerably longer to solve than convex quadratic programming (QP), but it is still possible to implement in online foot placement planning thanks to this discrete formulation.

*Remark.* This planner formulation is not limited to a specific type of terrain. Appropriate constraints and weights to represent different control objectives can be designed and implemented in a variety of flat-ground robotic walking scenarios.

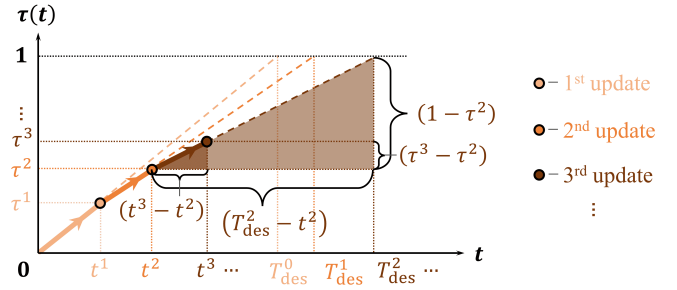


Fig. 3. Illustration of updating  $\tau(t)$  with respect to  $T_{des}^i$ . For instance, when  $T_{des}^2$  is updated at  $t^2$ ,  $\tau(t)$  becomes the linear function that starts from  $\tau^2$  and aims at 1 if  $t$  reaches  $T_{des}^2$ .

#### IV. ADAPTATION OF VARIABLE STEP DURATION IN THE LOW-LEVEL CONTROLLER

The foot placement planner in Section III updates the desired step position  $\mathbf{p}_{TD}^1$  and duration  $T^1$  of the next step at a low frequency during the current swing phase, while the low-level controller aims to regulate the robot's CoM dynamics towards the ALIP model and track a desired swing foot trajectory characterized by  $(\mathbf{p}_{TD}^1, T^1)$  at a high frequency (e.g., 25 Hz and 1 kHz respectively). In this work, we use an existing whole-body controller presented in [17] to track these task space outputs and maintain a stable walking gait. The outputs of the low-level controller are defined using the robot configuration  $q$  as

$$\mathcal{Y}^a(q) := \begin{pmatrix} \text{base height} \\ \text{torso orientation} \\ \text{swing foot position} \\ \text{swing foot orientation} \end{pmatrix}, \quad (11)$$

where the desired position of the swing foot is generated as a 3-D polynomial trajectory ending at the desired step position with the desired step duration.

Note that the low-level controller uses a dimensionless phase variable  $\tau$  to drive the trajectories of the robot, which increases monotonically from 0 to 1 during the current swing phase. If the step duration is fixed,  $\tau(t)$  is a linear function of the relative time  $t$  with a fixed slope. However, when the desired step duration is variable during the swing phase, we need to compute the phase variable  $\tau$  accordingly.

Let  $n$  be the number of times the planner updates the desired foot placement during a swing phase,  $t^i$  and  $\tau^i$  ( $i = \{0, 1, \dots, n\}$ ) be the relative timestamp and the phase variable at the  $i$ -th planner update. As the swing phase starting from  $t^0 = 0$  and  $\tau^0 = 0$ , the phase variable  $\tau(t)$  is designed as:

$$\tau(t) = \tau^i + (1 - \tau^i) \frac{t - t^i}{T_{des}^{1,i} - t^i}, \quad t \in [t^i, t^{i+1}], \quad (12)$$

where  $T_{des}^{1,i}$  is the  $i$ -th updated desired step duration. This design is primarily based on the following key points (See Fig. 3):

- 1)  $\tau(t)$  increases monotonically from 0 to 1 as  $t$  increases from 0 to the last updated desired step duration  $T_{des}^{1,n}$ ;

- 2)  $\tau(t)$  is continuous over  $t$  and piecewise linear in all  $[t^i, t^{i+1}]$ ;
- 3) In each  $[t^i, t^{i+1}]$ ,  $\tau(t)$  increases with a fixed slope such that it starts from  $\tau^i$  and aims to reach 1 if  $t$  reaches  $T_{des}^{1,i}$ , and then the slope is updated with the new  $T_{des}^{1,i+1}$  at  $t = t^{i+1}$ .

Moreover, the time derivative of the phase variable,  $\dot{\tau}(t)$ , is used to compute the time derivatives of the desired outputs  $\dot{y}^{des}$  inside the low-level controller, thus it can be computed using (12) as:

$$\dot{\tau}(t) = \frac{1 - \tau^i}{T_{des}^i - t^i}, \quad t \in [t^i, t^{i+1}]. \quad (13)$$

## V. SIMULATION RESULTS

This foot placement planner is tested on the humanoid robot model Digit in the MuJoCo simulation environment [18]. The simulation runs at a fixed time step of 1 ms, the same as the low-level controller. The foot placement planner runs every 40 ms (i.e., 40 simulation time steps) and the nonlinear MPC in the foot placement planner is solved using the open-source solver IPOPT [19]. To balance the planner performance and computational efficiency, we choose the number of future steps considered in the MPC as  $N = 4$ , which includes two complete cycles of 3-D bipedal walking. For all presented simulations, the parameters and constants of the foot placement planner are chosen as follows:

- The step position bound is defined as a rectangular area of dimension  $0.2 \times 0.1$  meters centered at each  $\mathbf{p}_{stone}^k$ ;
- The step duration has a nominal value  $T_{nom} = 0.5$  with the bound  $[T_{min}, T_{max}] = [0.35, 0.65]$  seconds;
- The initial DCM bounds are computed using the mechanical limits of the robot such as  $|x_{TD}^k| \leq 0.6$  and  $0.1 \leq |y_{TD}^k| \leq 0.5$  meters with the step duration bound;
- The cost weights for the  $k$ -th future step are chosen as  $\alpha_z^k, \alpha_u^k = [10, 000, 20, 000]$ ,  $\alpha_\sigma^k = 1$ , and  $\beta^k = 10^{4-k}$  for  $k = \{1, 2, 3, 4\}$ , where we double the weights in the  $y$ -direction because the step position bound in  $y$ -direction is half of that in  $x$ -direction.

For a comprehensive test of the planner performance, four types of stepping stone profiles and a perturbation scenario with four different perturbations are designed to represent the challenging terrain on the flat ground, where we compare our  $N$ -step preview planner (denoted as **ALIP-MPC**) with the one-step preview planner in [10] (denoted as **ALIP-QP**)<sup>1</sup>.

### A. Robust Walking on Stepping Stones

The stepping stone profiles are listed in Table I. Each profile contains 32 stones with each relative position computed using  $(L^j, W^j)$  as  $\mathbf{p}_{stone,rel}^j = [L^j, w_{l/r} + W^j]^T$  ( $j = \{1, \dots, 32\}$ ), where  $w_{l/r}$  is chosen as  $\pm 0.28$  meters.

In the simulation, the robot is initialized in a standing posture with zero velocity and then walks 6 steps to approach the first stepping stone. In this speeding-up stage, the robot

TABLE I  
STEPPING STONES PROFILES

Profile No.	$L^j$ (m)	$W^j$ (m)
I	fixed at $\{0.2, 0.4, 0.55\}$	fixed at $\{-0.15, 0.15\}$
II	$U[0.2, 0.5]$	$U[-0.15, 0.15]$
III	$(0.2*8, 0.5*8)*2$	$U[-0.15, 0.15]$
IV	$U[0.2, 0.5]$	$(-0.1*8, 0.1*8)*2$

Note: *Profile I* contains  $3 \times 2$  combinations of fixed  $L^j$  and  $W^j$ ; *Profile II-IV* includes one or two lists of uniformly distributed random values as  $L^j$  and/or  $W^j$ , denoted as  $U[\cdot, \cdot]$ ; *Profile III* uses a list of alternating values as  $L^j$ , which is 8 consecutive values of 0.2 followed by 8 values of 0.5 and repeated once, which emphasizes on abrupt changes of stone positions in the  $x$ -direction (similar to  $W^j$  in *Profile IV*).

TABLE II  
STEP POSITION ERRORS IN PROFILE I

$W^j \backslash L^j$	0.2	0.4	0.5
0.15	<b>0.036</b> 0.040	<b>0.020</b> 0.029	<b>0.028</b> N/A
-0.15	<b>0.039</b> 0.042	<b>0.019</b> 0.024	<b>0.022</b> N/A

Note: Comparison of step position errors (in meters) in the test of Profile I. ALIP-MPC outperforms ALIP-QP in these tests, where ALIP-QP fails in the tests of large step lengths with  $L^j = 0.55$  (m).

is only commanded to reach an appropriate  $x$ -velocity before walking onto the stepping stones with a right swing phase and thus may run into different initial conditions for the stepping stone test. Though such uncertainty helps highlight the robustness of our planner, we try to ensure consistent initial conditions in each comparison test between ALIP-MPC and ALIP-QP. As we will discuss below, ALIP-MPC outperforms ALIP-QP in all the presented simulation results.

1) *Profile I*: Table II lists the step position errors that are computed as the root-mean-square errors (RMSE) between the actual step positions and stone positions. For the test of  $L^j = 0.2$  and 0.4 meters, ALIP-MPC slightly reduces the step position errors compared to ALIP-QP. This is because these tests all lead to periodic gaits and thus the multi-step preview provides similar information as the one-step preview. However, in the test of  $L^j = 0.55$  meters, the desired step length becomes too large and close to the mechanical limit. ALIP-QP fails to maintain a viable gait starting from the first step onto the stepping stone due to the harsh initial condition, while ALIP-MPC completes all the tests thanks to the strategy that considers the viability of multiple future steps to decide the next foot placement.

2) *Profile II*: Each relative stone position is given by randomly generated  $(L^j, W^j)$ . ALIP-MPC completes this test with a step position error of 0.023 meters, while ALIP-QP ends halfway with the robot falling. Fig. 4 compares the footprints, the CoM, and the DCM trajectories of two planners. ALIP-QP fails at the 14th step because the 13th foot placement yields an initial condition that cannot lead to viable states given the 14th stone position, highlighting the significance of the multi-step preview. Fig. 5 compares the step duration and initial DCM in  $y$ -direction of two

<sup>1</sup>For animation video of the presented simulations, see <https://youtu.be/DjH69m1kbnM>.

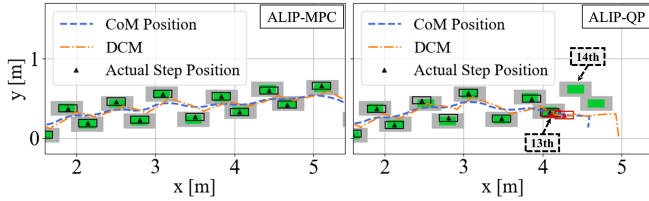


Fig. 4. Comparison of footprints in Profile II test. The black dots are the actual step positions, with the black frames illustrating the flat feet of the Digit, while the green rectangles mark the step position bounds on the gray stepping stones. (Left, ALIP-MPC) The robot walks stably through the random stones with a bounded DCM; (Right, ALIP-QP) The robot falls at the 14th step due to a non-viable foot placement of the 13th step (marked as red frames).

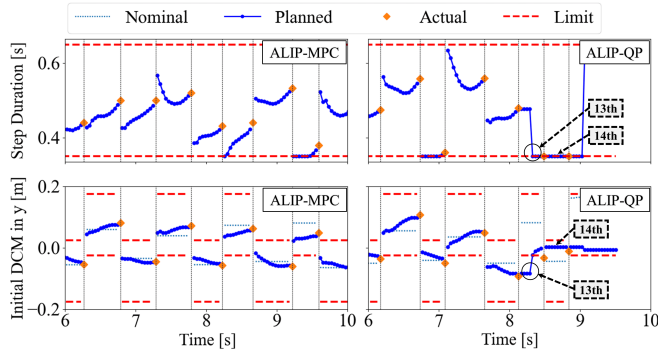


Fig. 5. Comparison of step duration and initial DCM in the test of Profile II. The vertical gray lines mark the touch-down moments of walking steps. (Left, ALIP-MPC) The step duration is adjusted to bound the DCM with smoother changes; (Right, ALIP-QP) ALIP-QP fails to bound the DCM.

planners, where ALIP-MPC can find foot placements to maintain viable states with smoother changes in the actual step duration.

3) *Profile III and IV*: These two profiles emphasize on the abrupt changes in the  $L^j$  and  $W^j$ , respectively. The step position errors of ALIP-MPC in these two tests are 0.027 and 0.024 meters, while ALIP-QP falls after a few steps. Fig. 6 shows the footprints of ALIP-MPC in both tests. Even under such challenging stepping stone profiles, especially with large variations in stone positions in the lateral direction, ALIP-MPC can find foot placements to maintain viable states.

### B. Perturbation Test on Stepping Stones

This test scenario contains 24 steps on the stepping stones profile  $(L^j, W^j) = (0.4, 0)$  meters and four force perturbations applied from all four directions to the pelvis of the Digit robot. Each perturbation force lasts from the relative time  $t = 0.1$  to 0.2 seconds in the specified step with the forces and directions as follows: 1) 5th step,  $F_x = 150$  N; 2) 10th step,  $F_x = -150$  N; 3) 15th step,  $F_y = 75$  N; 4) 20th step,  $F_y = -75$  N. The robot states during the perturbation test are plotted in Fig. 7. Since we choose a stone profile where the robot walks straightforwardly, the perturbation resistance of both planners in the  $x$ -direction is similar. When the first perturbation force pushes the robot forward, the robot takes the next step much faster than usual to keep balance

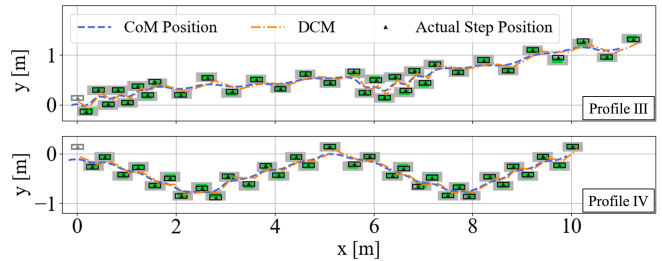


Fig. 6. Footprints of ALIP-MPC in the tests of Profile III (Upper) and Profile IV (Lower). The robot completes these tests without any step violating the step position constraint.

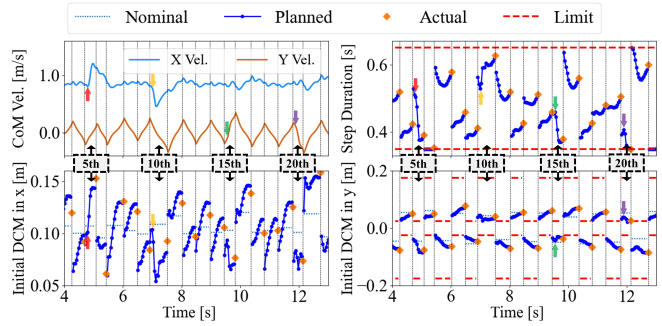


Fig. 7. Robot states of ALIP-MPC in the perturbation test. Four perturbation forces are marked by red, yellow, green, and purple arrows, respectively. (Upper Left) The  $x$ - and  $y$ -velocity changes abruptly due to the perturbation but is quickly restored; (Upper Right) The step duration is adjusted in response to the perturbation forces to maintain viable states; (Lower Left and Right) The initial DCM in both  $x$ - and  $y$ -direction are bounded.

(with increased CoM velocity and decreased step duration). The second push in the backward direction causes the robot to slow down and thus increases the step duration. In both tests, our approach demonstrates excellent capability of handling adversarial disturbances. When the push directions are orthogonal (i.e.,  $y$  direction) to the walking directions, the feasibility of viable steps is significantly reduced. The baseline ALIP-QP approach fails under disturbance, whereas the ALIP-MPC remains stable. This is because ALIP-MPC considers a longer horizon of locomotion, and therefore, is capable of regulating the durations of multiple future steps to improve stability and robustness.

## VI. CONCLUSION

This paper presents a discrete-time MPC formulation for multi-step preview foot placement planning with variable step duration. We demonstrate its performance of achieving more robust robotic walking on challenging terrains. Compared to other MPC formulations for stepping stones, the discrete dynamics of the initial DCM vastly simplify the optimization problem. However, due to the bilinear constraint in the optimization constraints, the average solving time of each iteration is around 30 to 50 ms. Future work will focus on improving the computational efficiency of the proposed approach and validating its effectiveness in real-world experiments. We will further develop more rigorous criteria for gait robustness on complex terrains.

## REFERENCES

- [1] Q. Nguyen, A. Agrawal, X. Da, W. C. Martin, H. Geyer, J. W. Grizzle, and K. Sreenath, "Dynamic walking on randomly-varying discrete terrain with one-step preview," in *Robotics: Science and Systems*, vol. 2, no. 3, 2017, pp. 384–99.
- [2] J. Li and Q. Nguyen, "Dynamic walking of bipedal robots on uneven stepping stones via adaptive-frequency mpc," *IEEE Control Systems Letters*, vol. 7, pp. 1279–1284, 2023.
- [3] S. Kajita, F. Kanehiro, K. Kaneko, K. Yokoi, and H. Hirukawa, "The 3d linear inverted pendulum mode: A simple modeling for a biped walking pattern generation," in *Proceedings 2001 IEEE/RSJ International Conference on Intelligent Robots and Systems. Expanding the Societal Role of Robotics in the the Next Millennium (Cat. No. 01CH37180)*, vol. 1. IEEE, 2001, pp. 239–246.
- [4] X. Xiong and A. D. Ames, "Orbit characterization, stabilization and composition on 3d underactuated bipedal walking via hybrid passive linear inverted pendulum model," in *2019 IEEE/RSJ International Conference on Intelligent Robots and Systems (IROS)*. IEEE, 2019, pp. 4644–4651.
- [5] R. Tedrake, S. Kuindersma, R. Deits, and K. Miura, "A closed-form solution for real-time zmp gait generation and feedback stabilization," in *Proc. IEEE-RAS Int. Conf. Humanoid Rob.*, 2015, pp. 936–940.
- [6] T. Sugihara, K. Imanishi, T. Yamamoto, and S. Caron, "3d biped locomotion control including seamless transition between walking and running via 3d zmp manipulation," in *Proc. IEEE Int. Conf. Rob. Autom.*, 2021, pp. 6258–6263.
- [7] T. Koolen, T. De Boer, J. Rebula, A. Goswami, and J. Pratt, "Capturability-based analysis and control of legged locomotion, part 1: Theory and application to three simple gait models," *The international journal of robotics research*, vol. 31, no. 9, pp. 1094–1113, 2012.
- [8] J. Engelsberger, C. Ott, and A. Albu-Schäffer, "Three-dimensional bipedal walking control based on divergent component of motion," *Ieee transactions on robotics*, vol. 31, no. 2, pp. 355–368, 2015.
- [9] R. J. Griffin and A. Leonessa, "Model predictive control for dynamic footstep adjustment using the divergent component of motion," in *2016 IEEE International Conference on Robotics and Automation (ICRA)*. IEEE, 2016, pp. 1763–1768.
- [10] M. Khadiv, A. Herzog, S. A. A. Moosavian, and L. Righetti, "Walking control based on step timing adaptation," *IEEE Transactions on Robotics*, vol. 36, no. 3, pp. 629–643, 2020.
- [11] R. Zhang, L. Meng, Z. Yu, X. Chen, H. Liu, and Q. Huang, "Stride length and stepping duration adjustments based on center of mass stabilization control," *IEEE/ASME Transactions on Mechatronics*, vol. 27, no. 6, pp. 5005–5015, 2022.
- [12] M.-J. Kim, D. Lim, G. Park, and J. Park, "Foot stepping algorithm of humanoids with double support time adjustment based on capture point control," in *2023 IEEE International Conference on Robotics and Automation (ICRA)*. IEEE, 2023, pp. 12 198–12 204.
- [13] Y. Gong and J. W. Grizzle, "Zero dynamics, pendulum models, and angular momentum in feedback control of bipedal locomotion," *Journal of Dynamic Systems, Measurement, and Control*, vol. 144, no. 12, p. 121006, 2022.
- [14] G. Gibson, O. Dosunmu-Ogunbi, Y. Gong, and J. Grizzle, "Terrain-adaptive, alip-based bipedal locomotion controller via model predictive control and virtual constraints," in *2022 IEEE/RSJ International Conference on Intelligent Robots and Systems (IROS)*. IEEE, 2022, pp. 6724–6731.
- [15] Y. Gao, Y. Gong, V. Paredes, A. Hereid, and Y. Gu, "Time-varying alip model and robust foot-placement control for underactuated bipedal robotic walking on a swaying rigid surface," in *2023 American Control Conference (ACC)*. IEEE, 2023, pp. 3282–3287.
- [16] P.-B. Wieber, "On the stability of walking systems," in *Proceedings of the international workshop on humanoid and human friendly robotics*, 2002.
- [17] G. A. Castillo, B. Weng, S. Yang, W. Zhang, and A. Hereid, "Template model inspired task space learning for robust bipedal locomotion," in *2023 IEEE/RSJ International Conference on Intelligent Robots and Systems (IROS)*. IEEE, 2023, pp. 8582–8589.
- [18] E. Todorov, T. Erez, and Y. Tassa, "Mujoco: A physics engine for model-based control," in *2012 IEEE/RSJ international conference on intelligent robots and systems*. IEEE, 2012, pp. 5026–5033.
- [19] A. Wächter and L. T. Biegler, "On the implementation of an interior-point filter line-search algorithm for large-scale nonlinear programming," *Mathematical programming*, vol. 106, pp. 25–57, 2006.